

Determining complementary properties with quantum clones

G.S. Thekkadath*, R.Y. Saaltink, L. Giner, and J.S. Lundeen
*Department of Physics, Centre for Research in Photonics,
University of Ottawa, 25 Templeton Street,
Ottawa, Ontario K1N 6N5, Canada
gthek044@uottawa.ca

In a classical world, simultaneous measurements of complementary properties (*e.g.* position and momentum) give a system's state. In quantum mechanics, measurement-induced disturbance is largest for complementary properties and, hence, limits the precision with which such properties can be determined simultaneously. It is tempting to try to sidestep this disturbance by copying the system and measuring each complementary property on a separate copy. However, perfect copying is physically impossible in quantum mechanics. Here, we investigate using the closest quantum analog to this copying strategy, optimal cloning. The coherent portion of the generated clones' state corresponds to "twins" of the input system. Like perfect copies, both twins faithfully reproduce the properties of the input system. Unlike perfect copies, the twins are entangled. As such, a measurement on both twins is equivalent to a simultaneous measurement on the input system. For complementary observables, this joint measurement gives the system's state, just as in the classical case. We demonstrate this experimentally using polarized single photons.

At the heart of quantum mechanics is the concept of complementarity: the impossibility of precisely determining complementary properties of a single quantum system. For example, a precise measurement of the position of an electron causes a subsequent momentum measurement to give a random result. Such joint measurements are the crux of Heisenberg's measurement-disturbance relation [1, 2], as highlighted by his famous microscope thought-experiment in 1927 [3]. Since then, methods for performing joint measurements of complementary properties have been steadily theoretically investigated [4–8], leading to seminal inventions such as heterodyne quantum state tomography [9, 10]. More recently, advances in the ability to control measurement-induced disturbance have led to ultra-precise measurements that surpass standard quantum limits [11], and also simultaneous determination of complementary properties with a precision that saturates Heisenberg's bound [12]. In sum, joint complementary measurements continue to prove useful for characterizing quantum systems [13–16] and for understanding foundational issues in quantum mechanics [11, 12, 17, 18].

In this Letter, we address the main challenge in performing a joint measurement, which is to circumvent the mutual disturbance caused by measuring two general non-commuting observables, \mathbf{X} and \mathbf{Y} . Classically, such joint measurements (*e.g.* momentum and position) are sufficient to determine the state of the system, even of statistical ensembles. In quantum mechanics, these joint measurements have mainly been realized by carefully designing them to minimize their disturbance, such as in weak [12–16, 18] or non-demolition [7, 11, 17] measurements. In order to avoid these technically complicated measurements, one might instead consider manipulating the system, and in particular, copying it. Subsequently, one would perform a standard measurement separately

on each copy of the system. Since the measurements are no longer sequential, or potentially not in the same location, one would not expect them to physically disturb one another. Crucially, as we explain below, the copies being measured must be correlated for this strategy to work. Hofmann recently proposed an experimental procedure that achieves this [19]. Following his proposal, we experimentally demonstrate that a partial-SWAP two-photon quantum logic gate [20] can isolate the measurement results of two photonic "twins". These twins are quantum-correlated (*i.e.* entangled) copies of a photon's polarization state that are ideal for performing joint measurements.

We begin by considering a physically impossible, but informative, strategy. Given a quantum system in a state ρ , consider making two perfect copies $\rho \otimes \rho$ and then measuring observable \mathbf{X} on copy one and \mathbf{Y} on copy two. In this case, the joint probability of measuring outcomes $X = x$ and $Y = y$ is $\text{Prob}(x, y) = \text{Prob}(x)\text{Prob}(y)$ [21]. Since it is factorable into functions of x and y , this joint probability cannot reveal correlations between the two properties. Even classically, this procedure would generally fail to give the system's state, since such correlations can occur in *e.g.* statistical ensembles. Less obviously, these correlations can occur in a single quantum system due to quantum coherence [4]. In turn, the lack of sensitivity to this coherence makes this joint measurement informationally incomplete [6], and thus this simplistic strategy is insufficient for determining quantum states [22]. Further confounding this strategy, the no-cloning theorem prohibits any operation that can create a perfect copy of an arbitrary quantum state, $\rho \rightarrow \rho \otimes \rho$ [23]. In summary, even if this strategy were allowed in quantum physics, it would not function well as a joint measurement.

Although perfect quantum copying is impossible, there

has been extensive work investigating “cloners” that produce imperfect copies [24]. Throughout this paper, we consider a general “1 → 2 cloner”. It takes as an input an unknown qubit state ρ_a along with a blank ancilla $\mathbf{I}_b/2$ (\mathbf{I} is the identity operator), and attempts to output two copies of ρ into separate modes, a and b .

We now consider a second strategy, one that utilizes a trivial version of this cloner by merely shuffling the modes of the two input states. This can be achieved by swapping their modes half of the time, and for the other half, leaving them unchanged. That is, one applies with equal likelihood the SWAP operation (\mathbf{S}_{ab} : $\rho_a \mathbf{I}_b/2 \rightarrow \mathbf{I}_a \rho_b/2$), or the identity operation ($\mathbf{I}_{ab} = \mathbf{I}_a \otimes \mathbf{I}_b$):

$$\rho_a \mathbf{I}_b/2 \rightarrow (\rho_a \mathbf{I}_b + \mathbf{I}_a \rho_b)/4 \equiv \mathbf{t}_{ab}. \quad (1)$$

Each output mode of the trivial cloner \mathbf{t}_{ab} contains an imperfect copy of the input state ρ . Jointly measuring \mathbf{X} and \mathbf{Y} , one on each trivial clone, yields the result $\text{Prob}(x, y) = (\text{Prob}(x) + \text{Prob}(y))/4$. In contrast to a joint measurement on perfect copies, this result exhibits correlations between x and y . These appear because in any given trial, only one of the observables is measured on ρ , while the other is measured on the blank ancilla. Hence, the apparent correlations are an artifact caused by randomly switching the observable being measured, and are not due to genuine correlations that could be present in ρ . While now physically allowed, this joint measurement strategy is still insufficient to determine the quantum state ρ .

In order to access correlations in the quantum state, we must take advantage of quantum coherence. Instead of randomly applying \mathbf{S}_{ab} or \mathbf{I}_{ab} as in trivial cloning, we require the superposition of these two processes, *i.e.* the coherent sum:

$$\mathbf{\Pi}_{ab}^j = \frac{1}{2}(\mathbf{I}_{ab} + j\mathbf{S}_{ab}), \quad (2)$$

where now we are free to choose the phase j . $\mathbf{\Pi}^j$ is a generalized symmetry operation that can implement a partial-SWAP gate [20]. For $j = +1$ (-1), this operation is a projection onto the symmetric (anti-symmetric) part of the trivial cloner input, $\rho_a \mathbf{I}_b/2$. The symmetric subspace only contains states that are unchanged by a SWAP operation. A projection onto this subspace increases the relative probability that ρ_a and the blank ancilla are identical. In fact, it has been proven that a symmetric projection on the trivial cloner input is the optimal cloning process, since it maximizes the fidelity of the clones (*i.e.* their similarity to ρ) [25–27].

This brings us to our third and final strategy. Optimal cloning achieves more than just producing imperfect copies: the clones are quantum-correlated, *i.e.* entangled [25]. This can be seen by examining the output state of the optimal cloner (*i.e.* with $j = 1$):

$$\sigma_{ab}^j = \frac{2}{3}(\mathbf{\Pi}_{ab}^j \rho_a \mathbf{I}_b \mathbf{\Pi}_{ab}^{j\dagger}) = \frac{2}{3}\mathbf{t}_{ab} + \frac{1}{3}\text{Re}[j\mathbf{c}_{ab}], \quad (3)$$

where $\mathbf{c}_{ab} = \mathbf{S}_{ab} \rho_a \mathbf{I}_b$ and $\text{Re}[\mathbf{s}] = (\mathbf{s} + \mathbf{s}^\dagger)/2$. While the first term is two trivial clones, the second term is the coherent portion of the optimal clones, and is the source of their entanglement. Considered alone, \mathbf{c}_{ab} corresponds to two “twins” of ρ . Like perfect copies, any measurement on either twin gives results identical to what would be obtained with ρ [19]. However, the twins are entangled. As such, it is important to realize that they are very different from the uncorrelated perfect copies we considered in the first strategy. Relative to these (*i.e.* $\rho \otimes \rho$), performing the same joint measurement as before, but on the twins \mathbf{c}_{ab} , provides more information about ρ . Measuring \mathbf{X} on one twin and \mathbf{Y} on the other yields the expectation value $\langle \mathbf{x}\mathbf{y} \rangle_\rho = \text{Tr}(\mathbf{x}\mathbf{y}\rho)$, where $\mathbf{x} = |x\rangle\langle x|$ and $\mathbf{y} = |y\rangle\langle y|$ are projectors onto the eigenstates of observables \mathbf{X} and \mathbf{Y} , respectively. Classically, this result would be interpreted as a joint probability $\text{Prob}(x, y)$. However, due to Heisenberg’s uncertainty principle, $\langle \mathbf{x}\mathbf{y} \rangle_\rho$ has non-classical features that shield precise determination of both \mathbf{X} and \mathbf{Y} . In fact, $\langle \mathbf{x}\mathbf{y} \rangle_\rho$ is a “quasiprobability” distribution much like the Wigner distribution [4], and has similar properties such as being rigorously equivalent to the state ρ [15]. Unlike the Wigner distribution, it is generally complex since $\mathbf{x}\mathbf{y}$ is not an observable (*i.e.* it is non-Hermitian). Although the measurements of \mathbf{X} and \mathbf{Y} are performed independently on each twin, because the twins are entangled, it is equivalent to simultaneously measuring the same two observables on a single copy of ρ . This approach is complementary to other joint measurement strategies for state determination in which the measurement itself is entangling, while the copies being measured are separable [28, 29].

Performing a joint measurement directly on twins cannot be achieved in a physical process. This is likely part of the reason why previous theoretical investigations concluded that optimal cloners were not ideal for joint measurements [25, 30, 31]. However, in a joint measurement on optimal clones, Hofmann showed that the contribution from the twins can be isolated from that of the trivial clones [19]. This is because changing the phase j affects only the coherent part of the cloning process. Thus, by adding joint measurement results obtained from the optimal cloner with different phases j , we can isolate the contribution from the twins and measure $\langle \mathbf{x}\mathbf{y} \rangle_\rho$ [32].

The experiment is shown schematically in Fig. 1. A photonic system lends itself to optimal cloning because the symmetry operation $\mathbf{\Pi}^j$ in Eq. 2 can be implemented with a beam splitter (BS). If two indistinguishable photons impinge onto different ports of BS1, Hong-Ou-Mandel interference occurs and the photons always “bunch” by exiting BS1 from a single port. By selecting cases where photons bunch (anti-bunch), one implements the symmetry projector $\mathbf{\Pi}^{+1}$ ($\mathbf{\Pi}^{-1}$) [33]. This enabled previous experimental demonstrations of optimal cloners for both polarization [34] and orbital angular momentum [35, 36] states. However, we must

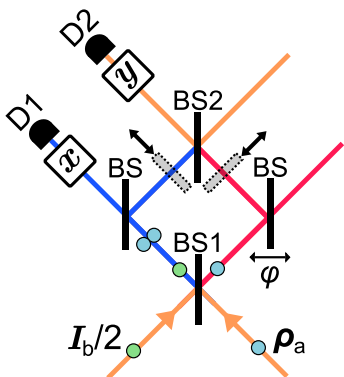


FIG. 1. **Schematic of experimental setup.** A photon in a polarization state ρ_a and a photon in a blank state $I_b/2$ enter an interferometer containing removable beam blocks (dotted outline). Complementary observables x and y are jointly measured by counting coincidences at detectors D1 and D2. When the red (blue) path is blocked, we post-select on the case where the photons exit the first beam splitter BS1 from the same (opposite) port and perform a symmetric projector Π^{+1} (anti-symmetric projector Π^{-1}), thus making two optimal clones of ρ . With no path blocked and a phase difference of $\varphi = \pm\pi/2$ between paths, we coherently combine both cases and perform $\Pi^{\pm i}$, respectively.

also implement $\Pi^{\pm i}$. Following a similar strategy as Refs. [20, 37], we use an interferometer to coherently combine the symmetric and anti-symmetric projectors, since $\Pi^{\pm i} = (e^{\pm i\pi/4}\Pi^{+1} + e^{\mp i\pi/4}\Pi^{-1})/\sqrt{2}$. This is achieved by interfering at BS2 the cases where the photons bunched at BS1 with cases where they anti-bunched at BS1. In summary, this provides an experimental procedure to vary the phase j and thereby isolate the joint measurement contribution of the twins from that of the trivial clones.

We experimentally verify that this procedure works by performing a joint measurement on trivial clones t_{ab} and showing that its outcome does not contribute to $\langle xy \rangle_\rho$. In particular, we scan the delay between ρ_a and $I_b/2$ at BS1. When the delay is zero, we implement the symmetry operator Π^j . When the delay is larger than the coherence time of the photons, the BS does not discriminate the symmetry of the two-qubit input state. Thus, it simply shuffles the modes of both qubits and produces trivial clones t_{ab} . We test the procedure by measuring $\langle xy \rangle_\rho = \langle dh \rangle_\rho$, where d and h are diagonal and horizontal polarization projectors, respectively. We use an input state $\rho_a = h$, for which one expects $\langle dh \rangle_\rho = \text{Tr}(dhh) = 0.5$. In Fig. 2, we show that for large delays $\langle dh \rangle_\rho = 0$, whereas for zero delay, it obtains its full value. This shows that the procedure has effectively removed the contribution of the trivial clones to the optimal clone state in Eq. 3, and so the joint measurement result is solely due to the twins.

A joint measurement on twins of ρ can reveal correlations between complementary properties in ρ . We

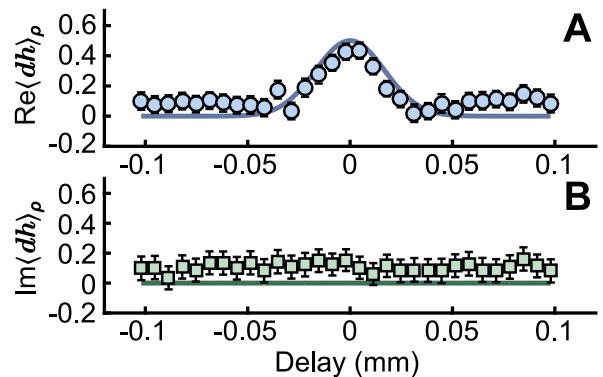


FIG. 2. **Transition from trivial to optimal cloning.** A horizontal photon $\rho_a = h$ is sent into the cloner. We jointly measure complementary observables d and h , one on each clone, and plot the real (A) and imaginary (B) parts of $\langle dh \rangle_\rho$. For large delays, only trivial clones are produced. Since they contain no information about $\langle dh \rangle_\rho$, our procedure cancels their contribution to the joint measurement result. At zero delay, optimal clones are produced. We isolate the contribution of the twins to the joint measurement, yielding the desired value of $\langle dh \rangle_\rho = 0.5$. The bold lines are theory curves calculated for intermediate delays [32]. Error bars are calculated using Poissonian counting statistics.

measure the entire joint quasiprobability distribution $\langle xy \rangle_\rho$ for the complementary polarization observables $x = \{d, a\}$ using diagonal and anti-diagonal projectors, and $y = \{h, v\}$ using horizontal and vertical projectors. This is repeated for a variety of different input states ρ . For the input state indicated by the dashed line in Fig. 3A, correlations can be seen in $\text{Im} \langle xy \rangle_\rho$, as shown in Fig. 3B. With the ability to exhibit correlations, $\langle xy \rangle_\rho$ is now a complete description of the quantum state ρ [32]. In particular, the wave function of the state (see Fig. 3A) is any cross-section of $\langle xy \rangle_\rho$. Moreover, the density matrix (see Fig. 3C) can be obtained with a Fourier transform of $\langle xy \rangle_\rho$. This is the key experimental result. In the classical world, simultaneously measuring complementary properties gives the system's state. This result demonstrates that simultaneously measuring complementary observables on twins, similarly, gives the system's state.

In addition to its fundamental importance, our result has potential practical advantages as a state determination procedure. It is valid for higher dimensional states [32] for which standard quantum tomography requires prohibitively many measurements. Specifically, a d -dimensional state typically requires $\mathcal{O}(d^2)$ measurements in $\mathcal{O}(d)$ bases to be reconstructed tomographically. In contrast, here the wave function is obtained directly (*i.e.* without a reconstruction algorithm) from $4d$ experimental measurements of only two observables, X and Y .

Our results uncover striking connections with other joint measurement techniques, despite the physics of each

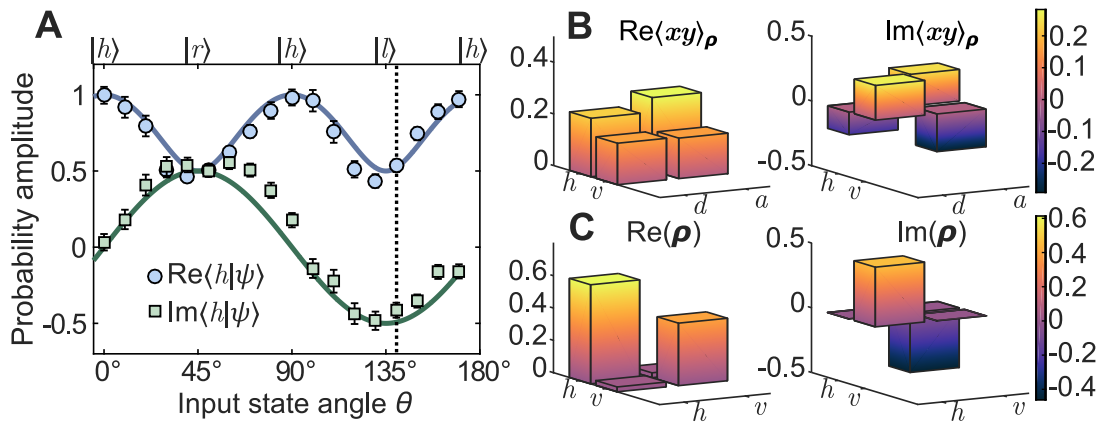


FIG. 3. **Measuring the quantum state.** Various polarization states $|\psi\rangle = \alpha|h\rangle + \beta|v\rangle$ are produced by rotating the fast-axis angle θ of a quarter-wave plate with increments of 10° . We plot the real and imaginary parts of $\alpha = \langle h|\psi\rangle = \sqrt{\frac{3}{8}} \cos(4\theta) + \frac{5}{8} + i \sin\theta \cos\theta$ in **A** (theory is bold lines, $|r\rangle = (|v\rangle + i|h\rangle)/\sqrt{2}$ and $|l\rangle = (|v\rangle - i|h\rangle)/\sqrt{2}$ are circular polarizations). Error bars are calculated using Poissonian counting statistics. The entire joint quasiprobability distribution (**B**) and density matrix (**C**) are also shown for the input state indicated by the dashed line (color represents amplitude). After processing the counts with a maximum-likelihood estimation, the average fidelity $|\langle \psi|\rho|\psi\rangle|^2$ of the 18 measured states is 0.92 ± 0.05 .

approach being substantially different. For example, the joint quasiprobability $\langle xy\rangle_\rho$ is also the average outcome of another joint measurement strategy: the weak measurement of y followed by a measurement of x on a single system ρ [15, 16, 19]. Furthermore, in the continuous-variable analogue of our work, measurements of complementary observables on cloned Gaussian states [38] give a different, but related, quasiprobability distribution for the quantum state known as the Q-function [10]. Finally, the result of a joint measurement on phase-conjugated Gaussian states can be used in a feedforward to produce optimal clones [39]. These connections emphasize the central role of optimal cloning in quantum mechanics [23, 27] and clarify the intimate relation between joint measurements of complementary observables and determining quantum states [4, 6].

We anticipate that simultaneous measurements of non-commuting observables can be naturally implemented in quantum computers using our technique, since the operation Π^j can be achieved using a controlled-SWAP quantum logic gate [19, 40]. As joint measurements are pivotal in quantum mechanics, this will have broad implications for state estimation [13–16], quantum control [17], and quantum foundations [12, 18]. For instance, we anticipate that our method can be used to efficiently and directly measure high-dimensional quantum states that are needed for fault-tolerant quantum computing and quantum cryptography [36].

This work was supported by the Canada Research Chairs (CRC) Program, the Natural Sciences and Engineering Research Council (NSERC), and Excellence Research Chairs (CERC) Program.

- [1] M. Ozawa, Phys. Lett. A **320**, 367 (2004).
- [2] P. Busch, P. Lahti, and R. F. Werner, Rev. Mod. Phys. **86**, 1261 (2014).
- [3] W. Heisenberg, Z. Phys. **43**, 172 (1927).
- [4] E. Wigner, Phys. Rev. **40**, 749 (1932).
- [5] E. Arthurs and J. L. Kelly, Bell Syst. Tech. J. **44**, 725 (1965).
- [6] W. M. de Muynck, P. A. E. M. Janssen, and A. Santman, Found. Phys. **9**, 71 (1979).
- [7] V. B. Braginsky, Y. I. Vorontsov, and K. S. Thorne, Science **209**, 547 (1980).
- [8] C. Carmeli, T. Heinosaari, and A. Toigo, Phys. Rev. A **85**, 012109 (2012).
- [9] J. Shapiro and S. Wagner, IEEE J. Quant. Electron. **20**, 803 (1984).
- [10] U. Leonhardt and H. Paul, Phys. Rev. A **47**, R2460 (1993).
- [11] G. Colangelo, F. M. Ciurana, L. C. Bianchet, R. J. Sewell, and M. W. Mitchell, Nature **543**, 525 (2017).
- [12] M. Ringbauer, D. N. Biggerstaff, M. A. Broome, A. Fedrizzi, C. Branciard, and A. G. White, Phys. Rev. Lett. **112**, 020401 (2014).
- [13] J. S. Lundeen, B. Sutherland, A. Patel, C. Stewart, and C. Bamber, Nature **474**, 188 (2011).
- [14] G. S. Thekkadath, L. Giner, Y. Chalich, M. J. Horton, J. Banker, and J. S. Lundeen, Phys. Rev. Lett. **117**, 120401 (2016).
- [15] C. Bamber and J. S. Lundeen, Phys. Rev. Lett. **112**, 070405 (2014).
- [16] J. Z. Salvail, M. Agnew, A. S. Johnson, E. Bolduc, J. Leach, and R. W. Boyd, Nat. Photon. **7**, 316 (2013).
- [17] S. Hacohe-Gourgy, L. S. Martin, E. Flurin, V. V. Ramesh, K. B. Whaley, and I. Siddiqi, Nature **538**, 491 (2016).
- [18] L. A. Rozema, A. Darabi, D. H. Mahler, A. Hayat, Y. Soudagar, and A. M. Steinberg, Phys. Rev. Lett.

- 109**, 100404 (2012).
- [19] H. F. Hofmann, Phys. Rev. Lett. **109**, 020408 (2012).
- [20] A. Černoč, J. Soubusta, L. Bartůšková, M. Dušek, and J. Fiurášek, Phys. Rev. Lett. **100**, 180501 (2008).
- [21] As is usual for a probability, $\text{Prob}(x, y)$ is estimated from repeated trials using an identical ensemble of input systems. This is implicit for probabilities and expectation values throughout the paper.
- [22] The strategy considered here is informationally equivalent to separating an identical ensemble into two and measuring $\text{Prob}(x)$ with one half and $\text{Prob}(y)$ with the other half. Knowing only these two marginal distributions is insufficient to determine the quantum state [42].
- [23] W. K. Wootters and W. H. Zurek, Nature **299**, 802 (1982).
- [24] V. Scarani, S. Iblisdir, N. Gisin, and A. Acín, Rev. Mod. Phys. **77**, 1225 (2005).
- [25] V. Bužek and M. Hillery, Phys. Rev. A **54**, 1844 (1996).
- [26] N. Gisin and S. Massar, Phys. Rev. Lett. **79**, 2153 (1997).
- [27] D. Bruss, A. Ekert, and C. Macchiavello, Phys. Rev. Lett. **81**, 2598 (1998).
- [28] J. Niset, A. Acín, U. L. Andersen, N. Cerf, R. García-Patrón, M. Navascués, and M. Sabuncu, Phys. Rev. Lett. **98**, 260404 (2007).
- [29] S. Massar and S. Popescu, Phys. Rev. Lett. **74**, 1259 (1995).
- [30] G. M. D’Ariano, C. Macchiavello, and M. F. Sacchi, J. Opt. B: Quantum Semiclass. Opt. **3**, 44 (2001).
- [31] T. Brougham, E. Andersson, and S. M. Barnett, Phys. Rev. A **73**, 062319 (2006).
- [32] See supplementary materials for details on the experimental setup, derivations, and some additional data. It also includes Ref. [41].
- [33] R. A. Campos and C. C. Gerry, Phys. Rev. A **72**, 065803 (2005).
- [34] W. T. M. Irvine, A. Lamas Linares, M. J. A. de Dood, and D. Bouwmeester, Phys. Rev. Lett. **92**, 047902 (2004).
- [35] E. Nagali, L. Sansoni, F. Sciarrino, F. De Martini, L. Marrucci, B. Piccirillo, E. Karimi, and E. Santamato, Nat. Photon. **3**, 720 (2009).
- [36] F. Bouchard, R. Fickler, R. W. Boyd, and E. Karimi, Science Adv. **3** (2017), 10.1126/sciadv.1601915.
- [37] J.-P. W. MacLean, K. Ried, R. W. Spekkens, and K. J. Resch, “Quantum-coherent mixtures of causal relations,” (2016), arXiv:1606.04523.
- [38] U. L. Andersen, V. Josse, and G. Leuchs, Phys. Rev. Lett. **94**, 240503 (2005).
- [39] M. Sabuncu, U. L. Andersen, and G. Leuchs, Phys. Rev. Lett. **98**, 170503 (2007).
- [40] R. B. Patel, J. Ho, F. Ferreyrol, T. C. Ralph, and G. J. Pryde, Science Adv. **2** (2016), 10.1126/sciadv.1501531.
- [41] T. Durt, B.-G. Englert, I. Bengtsson, and K. Życzkowski, Int. J. Quantum Inform. **8**, 535 (2010).
- [42] A. I. Lvovsky and M. G. Raymer, Rev. Mod. Phys. **81**, 299 (2009).

SUPPLEMENTARY MATERIAL

EXPERIMENTAL SETUP

A detailed figure containing the experimental setup is shown in Fig. S1. A 40 mW continuous-wave diode laser at 404 nm pumps a type-II β -barium borate crystal. Through spontaneous parametric down-conversion, pairs of 808 nm photons with orthogonal polarization are generated collinearly with the pump laser. The latter is then blocked by a long pass filter. The photon pair splits at a polarizing beam splitter (PBS), and each photon is coupled into a polarization-maintaining single mode fiber. The path length difference between the photon paths is adjusted with a delay stage. A spinning (2 Hz) half-wave plate produces a completely mixed state $I/2$ at one fiber output, while a half-wave plate and quarter-wave plate produce the state ρ to be cloned at the other fiber output. A displaced Sagnac interferometer composed of two BS is used instead of the interferometer in Fig. 1 (of main text), since it is more robust to air fluctuations and other instabilities. The phase φ between red and blue paths is adjusted by slightly rotating one of the mirrors in the interferometer in order to change the path length difference between both paths. A series of wave plates and a PBS are used to implement the projectors \mathbf{x} and \mathbf{y} . Detectors are single photon counting silicon avalanche photodiodes. Using time-correlation electronics, we count coincidence events that occur in a 5 nanosecond window and average over 60 seconds for each measurement.

JOINT MEASUREMENT ON OPTIMAL CLONES

For qudits, the d -dimensional observables \mathbf{X} and \mathbf{Y} are complementary if their eigenstates $\{|x\rangle\}$ and $\{|y\rangle\}$ all satisfy $|\langle x|y\rangle| = 1/\sqrt{d}$. We use the notation $\mathbf{x} = |x\rangle\langle x|$. The output of an optimal cloner for qudits is:

$$\sigma_{ab}^j = \frac{2}{d+1} \left(\Pi_{ab}^j \rho_a I_b \Pi_{ab}^{j\dagger} \right) \quad (\text{S4})$$

with $j = +1$. Consider measuring \mathbf{X} in mode a and \mathbf{Y} in mode b . As shown in Ref. [19], the joint probability of measuring outcome $X = x$ and $Y = y$ is:

$$\begin{aligned} \text{Prob}^j(x, y) &= \text{Tr} \left[\mathbf{x}_a \mathbf{y}_b \boldsymbol{\sigma}_{ab}^j \right] \\ &= \frac{1}{2(d+1)} \left(\langle \mathbf{x} \rangle_{\boldsymbol{\rho}} + \langle \mathbf{y} \rangle_{\boldsymbol{\rho}} + 2\text{Re} \left(j \langle \mathbf{x}\mathbf{y} \rangle_{\boldsymbol{\rho}} \right) \right). \end{aligned} \quad (\text{S5})$$

The terms $\langle \mathbf{x} \rangle_{\boldsymbol{\rho}}$ and $\langle \mathbf{y} \rangle_{\boldsymbol{\rho}}$ could be obtained from a joint measurement on trivial clones. In contrast, the last term $\langle \mathbf{x}\mathbf{y} \rangle_{\boldsymbol{\rho}}$ is obtained from a joint measurement on twins, and is a joint quasiprobability of simultaneously measuring both \mathbf{x} and \mathbf{y} on $\boldsymbol{\rho}$. In order to isolate the latter term, we use the fact that the joint measurement contribution of the trivial clones does not depend on the phase j , giving:

$$\langle \mathbf{x}\mathbf{y} \rangle_{\boldsymbol{\rho}} = \frac{d+1}{2} \sum_{j=\pm 1, \pm i} j^* \text{Prob}^j(x, y). \quad (\text{S6})$$

When the input state is pure, that is $\boldsymbol{\rho} = |\psi\rangle\langle\psi|$, then $\langle \mathbf{x}\mathbf{y} \rangle_{\psi} = \nu \langle y|\psi\rangle$, where $\nu = \langle \psi|x\rangle\langle x|y\rangle$. For some $x = x_0$, the phase of ν is constant for all y and so the wave function $|\psi\rangle$ can be expressed in the basis of \mathbf{Y} as $|\psi\rangle = \frac{1}{\nu} \sum_y \langle \mathbf{x}_0 \mathbf{y} \rangle_{\psi} |y\rangle$. As usual, the constant ν is found by normalizing $|\psi\rangle$. Thus, using Eq. S6, any complex amplitude $\psi(y) = \langle y|\psi\rangle$ of the wave function can be found from:

$$\psi(y) = \frac{d+1}{2\nu} \sum_{j=\pm 1, \pm i} j^* \text{Prob}^j(x_0, y). \quad (\text{S7})$$

The choice of x_0 is equivalent to choosing a phase reference for the wave function. In Fig. 3A of the main text, we use $x_0 = d$, which defines the diagonal polarization as $|d\rangle = (|h\rangle + |v\rangle)/\sqrt{2}$. We choose to make the normalization constant ν a real number, *i.e.* $\nu = (|\langle d|h\rangle|^2 + |\langle d|v\rangle|^2)^{1/2}$.

For mixed input states, the joint quasiprobability $\langle \mathbf{x}\mathbf{y} \rangle_{\boldsymbol{\rho}}$ is related to the density matrix $\boldsymbol{\rho}$ via a discrete Fourier transform (see derivation below).

RELATING THE JOINT QUASIPROBABILITY TO THE DENSITY MATRIX

Here we summarize the connection between the joint quasiprobability distribution and the density matrix. Consider the d -dimensional complementary observables \mathbf{X} and \mathbf{Y} with eigenstates $\{x_i\}$ and $\{y_j\}$ such that $|\langle x_i|y_j\rangle| = 1/\sqrt{d}$ for any i, j . Without loss of generality [41], one can take the $\{y_i\}$ basis to be defined in terms of a discrete Fourier transform of $\{x_i\}$: $|y_j\rangle = \sum_{i=0}^{d-1} |x_i\rangle \exp(i2\pi x_i y_j/d)/\sqrt{d}$. This fixes a phase relation for the inner product of all the eigenstates of both bases:

$$\langle x_i|y_j\rangle = \exp(i2\pi x_i y_j/d)/\sqrt{d}. \quad (\text{S8})$$

A general d -dimensional quantum state $\boldsymbol{\rho}$ can be written in the basis of \mathbf{Y} as $\boldsymbol{\rho} = \sum_{k,l} p_{kl} |y_k\rangle\langle y_l|$. We wish to relate the coefficients p_{kl} to the joint quasiprobability distribution described in the main text, *i.e.* $\langle \mathbf{x}\mathbf{y} \rangle_{\boldsymbol{\rho}}$. Recall that we use the notation $\mathbf{x} = |x\rangle\langle x|$. Thus $\langle \mathbf{x}\mathbf{y} \rangle_{\boldsymbol{\rho}}$ takes the form of $D_{ij} \equiv \langle |x_i\rangle\langle x_i|y_j\rangle\langle y_j| \rangle_{\boldsymbol{\rho}} = \text{Tr} [|x_i\rangle\langle x_i|y_j\rangle\langle y_j| \boldsymbol{\rho}] = \langle x_i|y_j\rangle\langle y_j|\boldsymbol{\rho}|x_i\rangle$. Inserting the expanded form of $\boldsymbol{\rho}$:

$$D_{ij} = \langle x_i|y_j\rangle\langle y_j| \sum_{k,l} p_{kl} |y_k\rangle\langle y_l| \langle y_l|x_i\rangle = \langle x_i|y_j\rangle \sum_l p_{jl} \langle y_l|x_i\rangle = \frac{\exp(i2\pi x_i y_j/d)}{d} \sum_{l=0}^{d-1} p_{jl} \exp(-i2\pi x_i y_l). \quad (\text{S9})$$

This shows that the joint quasiprobability is the discrete Fourier transform of the density matrix. The equation can be inverted by taking the inverse Fourier transform of both sides:

$$p_{jl} = \sum_{i=0}^{d-1} D_{ij} \exp(i2\pi x_i(y_l - y_j)). \quad (\text{S10})$$

In the case of polarization qubits, $\mathbf{x} = \{\mathbf{d}, \mathbf{a}\}$ and $\mathbf{y} = \{\mathbf{h}, \mathbf{v}\}$. Then the equation relating the two density matrix and the joint quasiprobability is:

$$\boldsymbol{\rho} = \begin{pmatrix} \langle d|h \rangle_{\boldsymbol{\rho}} + \langle a|h \rangle_{\boldsymbol{\rho}} & \langle d|h \rangle_{\boldsymbol{\rho}} - \langle a|h \rangle_{\boldsymbol{\rho}} \\ \langle d|v \rangle_{\boldsymbol{\rho}} - \langle a|v \rangle_{\boldsymbol{\rho}} & \langle d|v \rangle_{\boldsymbol{\rho}} + \langle a|v \rangle_{\boldsymbol{\rho}} \end{pmatrix}. \quad (\text{S11})$$

Eq. S11 is used to calculate the density matrix in Fig. 3C of the main text.

TRIVIAL TO OPTIMAL CLONES

When the two input photons are temporally distinguishable, Hong-Ou-Mandel interference does not occur at the first beam splitter, and the cloner produces trivial clones t_{ab} . Conversely, for temporally indistinguishable photons, we produce σ_{ab}^j . Photons that are partially distinguishable can be decomposed into the form

$$\sigma_{ab}^j = |\alpha|^2 \sigma_{ab}^j + (1 - |\alpha|^2) t_{ab}, \quad (\text{S12})$$

where $\alpha \in [0, 1]$ is a temporal distinguishability factor. In particular, the temporal mode of the delayed photon in mode a can be written as $|\zeta_a\rangle = \int d\omega \phi(\omega) e^{-i\omega\tau} a^\dagger(\omega) |0\rangle$ where τ is the delay, while the other photon in mode b is described by $|\zeta_b\rangle = \int d\omega \phi(\omega) b^\dagger(\omega) |0\rangle$. For a Gaussian spectral amplitude $\phi(\omega) = \frac{1}{\sqrt{\pi\Delta\omega}} e^{-\frac{(\omega-\omega_0)^2}{2\Delta\omega^2}}$ where ω_0 is the central frequency of the photons and $\Delta\omega$ is their spectral width, the distinguishability factor is given by

$$|\alpha|^2 = |\langle \zeta_a | \zeta_b \rangle|^2 = e^{-\frac{\Delta\omega^2 \tau^2}{2}}. \quad (\text{S13})$$

In the experiment, we adjust the delay τ by moving the delay stage. The parameter $\Delta\omega^2$ is extracted from fitting a Gaussian to the Hong-Ou-Mandel dip (see Fig. S2).

EXTENDED DATA

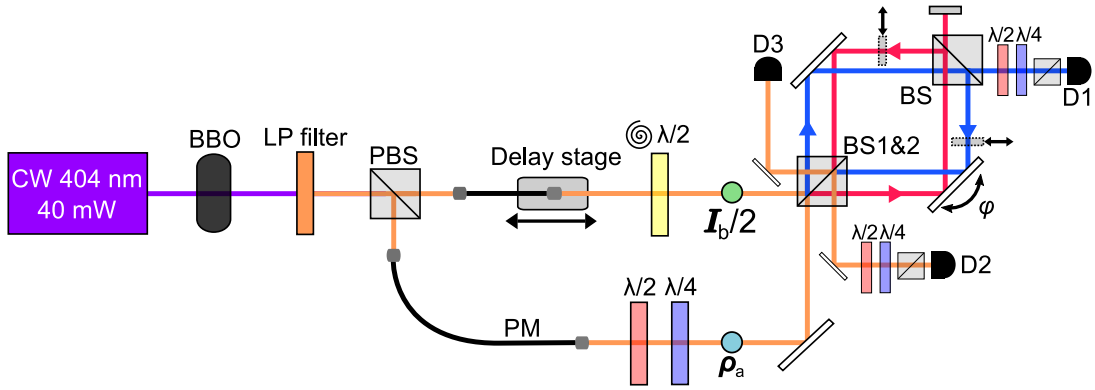


FIG. S4. **Experimental setup.** Details of the experimental setup can be found in the Methods section. A simplified schematic of this setup is shown in the main text. Detector D3 is used for alignment purposes, but otherwise is not used in the experiment. CW: continuous-wave, BBO: β -barium borate, LP: long pass, (P)BS: (polarizing) beam splitter, PM: polarization-maintaining, $\lambda/2$: half-wave plate, $\lambda/4$: quarter-wave plate, D: avalanche photodiode detector.

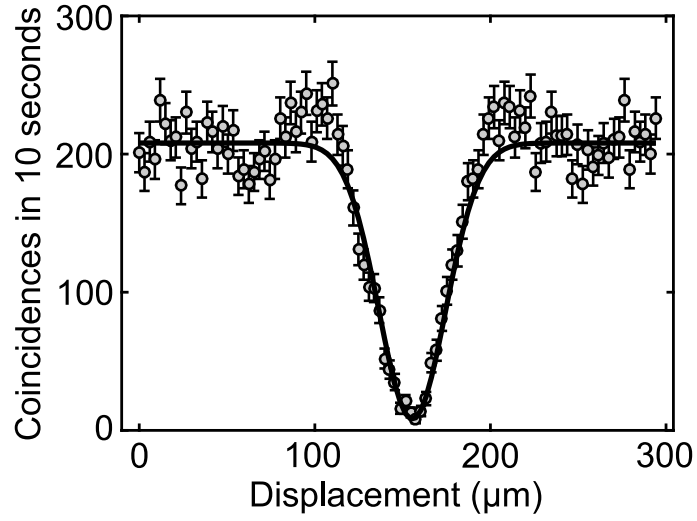


FIG. S5. **Hong-Ou-Mandel interference.** In order to characterize the spectral width of the photons and to ensure that we are performing the symmetry projector $\Pi_{ab}^{\pm 1}$, we measure the width and visibility of the Hong-Ou-Mandel dip at BS1. With both input photons horizontally polarized and the blue path blocked, we measure the number of coincidences at detectors D1 and D2 as a function of the position of the delay stage. The visibility $\mathcal{V} = (C_{max} - C_{min}) / (C_{max} + C_{min})$ (where C is the number of coincidences) of the dip is $\sim 96\%$. Error bars are calculated using Poissonian counting statistics.

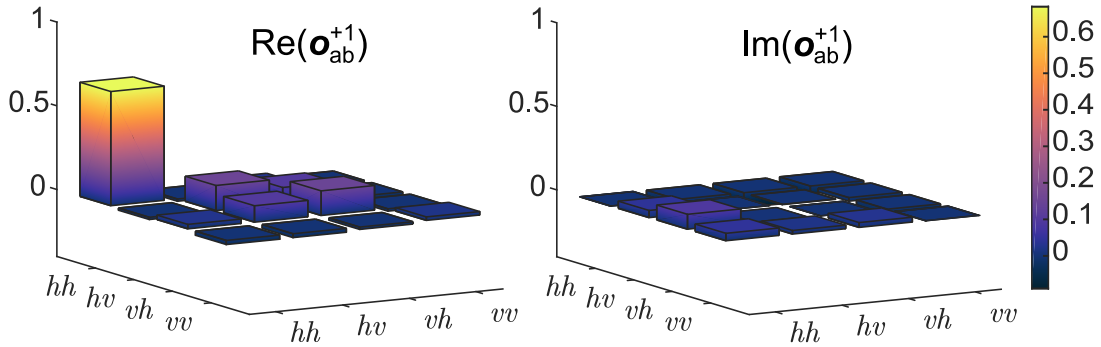


FIG. S6. **Quantum state tomography of Π_{ab}^{+1} output.** In order to determine the fidelity of our clones, we perform two-photon quantum state tomography on the output \mathbf{o}_{ab}^{+1} of the cloner. Here the input state to be cloned is $\rho_a = \mathbf{h}$. By tracing over each subsystem of the measured \mathbf{o}_{ab}^{+1} , we can compute the fidelities $F_a = |\langle \mathbf{h} | \mathbf{o}_a^{+1} | \mathbf{h} \rangle|^2$ and $F_b = |\langle \mathbf{h} | \mathbf{o}_b^{+1} | \mathbf{h} \rangle|^2$. We obtain $F_a = 0.832$ and $F_b = 0.829$, which nearly saturates the theoretical bound of $5/6 \sim 0.833$.

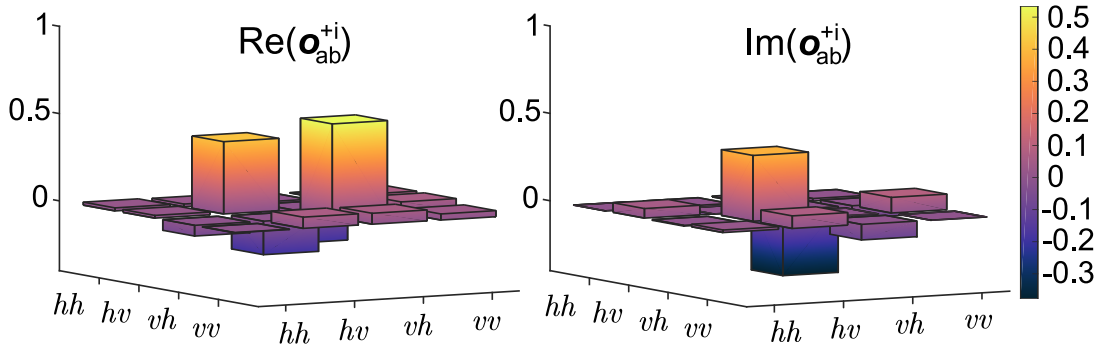


FIG. S7. **Quantum state tomography of Π_{ab}^{+i} output.** In order to achieve the Π_{ab}^{+i} operation, both paths in the interferometer are unblocked and the phase between them is $\varphi = \pi/2$. We test our ability to implement Π_{ab}^{+i} by performing two-photon quantum state tomography on the state after the Π_{ab}^{+i} operation. As an input, we use the state $|\mathbf{h}\mathbf{v}\rangle\langle\mathbf{h}\mathbf{v}|$. In this case, the fidelity of the output state \mathbf{o}_{ab}^{+i} is 0.850.

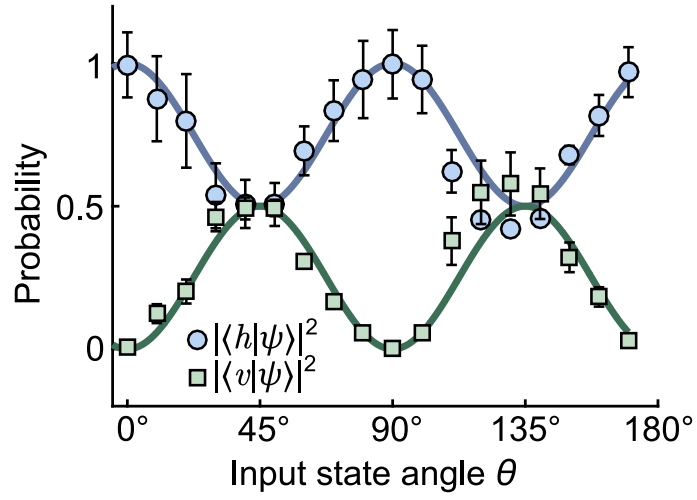


FIG. S8. **Absolute value squared of the measured wave function.** The data in this figure is the same as the data used in Fig. 3 of the main text. The polarization state of the input photon as a function of the the quarter wave-plate fast-axis can be written in the form $|\psi\rangle = \alpha|h\rangle + \beta|v\rangle$. Here we plot both $|\alpha|^2 = \cos^4\theta + \sin^4\theta$ and $|\beta|^2 = 2\sin^2\theta\cos^2\theta$ (theory is bold lines). Error bars are calculated using Poissonian counting statistics.